Journal of the American College of Cardiology
© 2003 by the American College of Cardiology Foundation
Published by Elsevier Inc.

Vol. 42, No. 8, 2003
ISSN 0735-1097/03/$30.00
doi:10.1016/S0735-1097(03)01034-9

Cardiac Imaging

Time Interval Between Onset of Mitral Inflow and Onset of Early Diastolic Velocity by Tissue Doppler: A Novel Index of Left Ventricular Relaxation

Experimental Studies and Clinical Application

Carlos Rivas-Gotz, MD, Dirar S. Khoury, PHD, Michael Manolios, MD, Liyun Rao, PHD, Helen A. Kopelen, RDCS, Sherif F. Nagueh, MD

Houston, Texas

OBJECTIVES The goal of this study was to examine the diagnostic utility of the time to onset of early (Ea) diastolic velocity of the mitral annulus by tissue Doppler (TD) in comparison with the time to onset of mitral inflow (T_{Ea-E}) for the assessment of left ventricular (LV) relaxation.

BACKGROUND Tissue Doppler imaging of the mitral annulus provides useful information about myocardial function. So far, studies have focused on the measurement of peak Ea, but have not evaluated the diagnostic utility of the time to onset of Ea.

METHODS Simultaneous left heart catheterization and Doppler echocardiography (DE) were performed in 10 dogs. Left atrial pressures and LV volumes and pressures were measured before and after constriction of the circumflex (cx) coronary artery. The delay in Ea was next examined in 60 consecutive patients, undergoing simultaneous right heart catheterization and DE. Furthermore, (T_{Ea-E}) was used to predict filling pressures in a prospective group of 33 patients.

RESULTS In canine studies, significant prolongation in the time interval (T_{Ea-E}) was noted after cx constriction, which had a significant relation with tau (τ) ($r = 0.93$, $p < 0.01$). In human studies, Ea was significantly delayed in patients with impaired relaxation and pseudonormal LV filling in comparison with age-matched controls. In the prospective group, pulmonary capillary wedge pressure (PCWP) derived as: $PCWP_{Doppler} = LV_{end\text{-}systolic\ pressure} \times e^{-IVRT/(T_{Ea-E})}$, where IVRT is isovolumetric relaxation time; $PCWP_{Doppler}$ related well to $PCWP_{catheter}$ ($r = 0.84$, $p < 0.001$).

CONCLUSIONS T_{Ea-E} is a useful novel index of LV relaxation. It can be used to identify patients with diastolic dysfunction and predict PCWP. (J Am Coll Cardiol 2003;42:1463–70) © 2003 by the American College of Cardiology Foundation

Tissue Doppler (TD) imaging is a valuable technique for the assessment of left ventricular (LV) regional and global function (1,2). The evaluation of myocardial diastolic signals along the long axis of the LV at the level of the mitral annulus is particularly useful for the determination of LV relaxation and filling pressures (3–9). Most of the available studies have primarily focused on the measurement of the early (Ea) and late (Aa) diastolic velocities. However, Ea is load-dependent in the absence of cardiac disease (8). Therefore, its application can result in erroneous conclusions about LV relaxation in normal subjects with reduced left atrial (LA) pressures. An important, but yet unexplored, parameter could be obtained from the TD signals, namely the onset of Ea and its relation to the onset of transmitral inflow. An earlier study (9) noted that, in patients with restrictive cardiomyopathy, the peak velocity of Ea occurs after that of transmitral early diastolic velocity (mitral E), whereas in normal individuals they occur almost simultaneously. Similar observations were recently reported in an animal model of pacing-induced heart failure (10). The hemodynamic reasons for this observation and the potential clinical application to the evaluation of LV diastolic function remain unknown. We underwent this study to evaluate this time interval in canine experiments where we induced myocardial dysfunction and related it to indexes of LV relaxation. Then we tested the utility of this time interval in the clinical setting to identify patients with impaired LV relaxation across a wide range of filling pressures. Furthermore, we validated its use for determining wedge pressure in a prospective population.

See page 1471

METHODS

Canine experiments. ANIMAL PREPARATION. After the Baylor College of Medicine Animal Research Committee approved the study, 10 healthy adult mongrel dogs were anesthetized with sodium pentobarbital (30 mg/kg), intubated, and mechanically ventilated with an external respi-

From the Section of Cardiology, Department of Medicine, Baylor College of Medicine, Houston, Texas. Supported by a Scientist Development Grant to Dr. Nagueh (0030235N) from the American Heart Association, National Center, Dallas-Texas, and by HL68768 (to D.S.K.) from the NIH, Bethesda, Maryland.

Manuscript received December 17, 2002; revised manuscript received May 12, 2003, accepted June 15, 2003.

JACC Vol. 42, No. 8, 2003
October 15, 2003:1463–70

Abbreviations and Acronyms

Aa	= late diastolic velocity by tissue Doppler
Ea	= early diastolic velocity by tissue Doppler
EDV	= end-diastolic volume
EDP	= end-diastolic pressure
IVC	= inferior vena cava
IVRT	= isovolumetric relaxation time
LA	= left atrium or atrial
LV	= left ventricle/left ventricular
PCWP	= pulmonary capillary wedge pressure
TD	= tissue Doppler
T_{Ea-E}	= time interval between onset of Ea and onset of mitral inflow

rator. After a midline sternotomy, the heart was exposed, and a pair of pacing electrodes was sutured to the right atrial appendage. Then, to depress its rate of spontaneous depolarization, the sinus node was modified by radiofrequency energy with an epicardial approach. This allowed control of the ventricular rate while maintaining native atrioventricular conduction. After calibration, a high fidelity 5F pressure catheter (Millar Instruments, Houston, Texas) was introduced into the LA through its appendage. Likewise, to measure LV volumes and pressures, a calibrated 5F 12-electrode conductance catheter (Millar) was advanced into the LV by crossing the aortic valve (positioned along LV long axis). The latter catheter was connected to a dedicated system (Cardiodynamics BV, Leycom-CFL- 512, Argonstraat, the Netherlands) that continuously acquired and displayed pressure, volume, and electrocardiogram signals. Using fluoroscopic guidance, a pulmonary artery (Swan-Ganz) catheter was advanced from the right femoral vein to the pulmonary circulation.

Further, to alter myocardial function, an arterial constrictor was placed around the proximal segment of the left circumflex coronary artery, and an ultrasonic flow transducer was placed distal to the arterial constriction. Also, the inferior vena cava (IVC) was dissected, and a ring was placed around it to allow for gradual occlusion of the vein.

HEMODYNAMIC MEASUREMENTS. To convert the conductance signals to volume data, blood resistivity was measured using the CFL-512 system; cardiac output was simultaneously acquired by both the conductance and pulmonary artery catheters, and parallel conductance was derived by injecting 10 ml of hypertonic saline into the pulmonary artery through the distal port of the pulmonary artery catheter.

All recordings of pressure and volume data were obtained at end-expiration. Left ventricular minimal and end-diastolic (EDP) pressures were measured. Left ventricular volume at end diastole (EDV) was obtained from the conductance catheter (11). Tau was also calculated (12). Using the pressure-volume loops, end-systolic elastance (Ees) (slope of the end-systolic pressure:end-systolic volume relationship) was derived. Left atrium "v" pressure and the early diastolic transmitral pressure gradient were also determined.

ECHOCARDIOGRAPHY. The animals were imaged from the epicardium using an ultrasound system equipped with TD imaging capability. In the apical four-chamber view, pulse wave Doppler was applied to record mitral inflow at the valve tips (intraobserver variability for measuring mitral peak E velocity: 3 ± 1%). Tissue Doppler program was applied in PW Doppler to record mitral annular velocities at the septal, anterior, inferior, and lateral areas (5). The peak velocity of Ea (intraobserver variability 5 ± 2%) at above sites of the annulus was measured under the different loading conditions, including before and after circumflex constriction. The time intervals between the peak of R wave and onset of mitral E velocity and between peak of R wave and onset of Ea at the four areas of the mitral annulus were measured. Subsequently, the difference between these time intervals (T_{Ea-E}) was calculated for each of the four areas, and an average value was derived (intraobserver variability 4 ± 2%, interobserver variability 6 ± 2%).

EXPERIMENTAL PROTOCOL. Throughout the experimental protocol, LV hemodynamics were allowed to equilibrate for 5 to 10 min before recording the changes. After acquiring baseline data, IVC occlusion was performed to decrease LV volumes and pressures, with subsequent reacquisition of hemodynamic and Doppler data at the new loading conditions. Next, the proximal segment of the left circumflex coronary artery was constricted until coronary artery blood flow decreased by ≥90%. Again, hemodynamic and echocardiographic studies were performed before and after IVC occlusion.

Human studies. INITIAL GROUP. The institutional review board of Baylor College of Medicine approved the protocol, and all patients provided written informed consent. The group was comprised of 60 consecutive patients who were undergoing right heart catheterization in the cardiac catheterization laboratory (n = 25) or the intensive care unit (n = 35). Inclusion criteria were sinus rhythm (60 to 100 beats/min); satisfactory Doppler and pressure recordings; and absence of mitral stenosis, prosthetic mitral valve, and severe mitral regurgitation. Patients had simultaneous echocardiographic and hemodynamic measurements.

ECHOCARDIOGRAPHIC STUDIES. Patients were imaged in a supine position with an ultrasound system equipped with harmonic imaging, a multifrequency transducer, and TD imaging capability. After acquiring parasternal and apical views, pulse-Doppler was utilized to record transmitral and pulmonary venous flow in the apical four-chamber view as previously described (13). Tissue Doppler imaging was applied in the PW mode to record the mitral annular velocities at the septal, lateral, inferior, and anterior areas. Studies were recorded for later playback and analysis.

ECHOCARDIOGRAPHIC ANALYSIS. The analysis was performed offline without knowledge of hemodynamic data.

Table 1. Effect of Cx Stenosis and IVC Occ. in Canine Experiments

	Baseline	IVC Occ. 1	Cx Stenosis	IVC Occ. 2
LA v pressure (mm Hg)	10.5 ± 4	5.3 ± 3†	13.5 ± 3*	6.7 ± 2.5‡
Heart rate (beats/min)	112 ± 6	110 ± 6	112 ± 7	113 ± 7
EDP (mm Hg)	5 ± 2	2.5 ± 1.7†	9 ± 2*	4.7 ± 2.1§
LV minimal pressure (mm Hg)	1 ± 0.4	0.6 ± 0.2†	4.5 ± 0.7*	2.7 ± 1‡
TMG (mm Hg)	8.7 ± 3	5.9 ± 2†	6.5 ± 2*	3.5 ± 1.5‡
EDV (ml)	53 ± 8	27 ± 5†	65 ± 7*	32 ± 7†
Tau (ms)	36 ± 4	32 ± 3	46 ± 4*	37 ± 3
Ees (mm Hg/ml)	5 ± 0.7		2.3 ± 0.8†	
Average Ea (cm/s)	6 ± 2	3 ± 1.5†	4.5 ± 1.5‡	4.1 ± 1.7‡
Average ($T_{Ea\text{-}E}$) (ms)	0 ± 4	3 ± 5	29 ± 5‡	25 ± 4‡

*$p < 0.05$ vs. baseline IVC occlusion 1 and 2; †$p < 0.05$ vs. baseline; ‡$p < 0.05$ vs. baseline and IVC occlusion 1; §$p < 0.05$ vs. IVC occlusion 1.

Cx = circumflex; Ea = early diastolic velocity by tissue Doppler; EDP = end-diastolic pressure; EDV = end-diastolic volume; IVC = inferior vena cava; LA = left atrium; LV = left ventricle; Occ. = occlusion; $T_{Ea\text{-}E}$ = time interval between onset of Ea and onset of mitral inflow.

Left ventricular EDV, ejection fraction, and LA maximum volume were performed per the recommendations of the American Society of Echocardiography (14). All Doppler values represent the average of three beats. Mitral inflow was analyzed for peak E, peak A velocities, E/A ratio, deceleration time of E velocity, and isovolumetric relaxation time (IVRT) (interobserver variability 4 ± 2%). From the pulmonary vein flow velocities (feasible in 35 patients), the systolic filling fraction was computed (15), and the difference between Ar and transmitral A velocity duration was calculated (Ar-A duration) (16). The Ea and Aa velocities at the four areas of the mitral annulus were measured, and the dimensionless ratio E/Ea (5–7) was computed (septal, lateral, and average).

In addition, similar to the canine experiments, the time intervals between peak of R wave and onset of mitral E velocity as well as the time interval between peak of R wave and onset of Ea at the four areas of the mitral annulus were measured. The R-R intervals used for timing the onset of mitral E and TD Ea were identical. Subsequently, the $T_{Ea\text{-}E}$ (interobserver variability 5 ± 2%) was computed at the four areas, and an average value was derived. The $T_{Ea\text{-}E}$ was then used to predict pulmonary capillary wedge pressure (PCWP) using the equation (17): $PCWP = LV_{es} \times e^{-IVRT/(T_{Ea\text{-}E})}$, where $LV_{es} = 0.9 \times$ aortic systolic pressure (18).

HEMODYNAMIC MEASUREMENTS. Hemodynamic data were collected by an investigator unaware of the echocardiographic measurements at end expiration and represent the average of five cycles. Cardiac output was derived by the thermodilution technique (average of three cardiac cycles with <10% variation). All pressures including PCWP (wedge verified by fluoroscopy, phasic changes in pressure waveforms, and oxygen saturation) were determined using balanced transducers (0 level at midaxillary line). Tau was computed in the initial population using the previously validated equation $Tau = IVRT/(Ln\ LVS - Ln\ PCWP)$ (17), where IVRT was measured by Doppler, and LVS and PCWP were obtained by invasive measurements, and Ln means natural logarithm and LVS means left ventricular end-systolic pressure.

PROSPECTIVE POPULATION. The utility of the time interval $T_{Ea\text{-}E}$ to predict filling pressures was also examined in a prospective group of 33 (15 patients in the catheterization laboratory) consecutive patients who had simultaneous Doppler and right heart catheterization.

Statistical analysis. The hemodynamic and Doppler studies were compared in the four experimental stages of the canine experiments using repeated measures analysis of variance (ANOVA) with paired comparisons (baseline vs. each of: IVC occlusion [one], circumflex stenosis and IVC occlusion [two], IVC occlusion [one] vs. each of circumflex stenosis and IVC occlusion [two], and circumflex stenosis vs. IVC occlusion [two]) performed using Bonferroni *t* test. For the human studies, the initial population of 60 patients was divided based on echocardiographic and hemodynamic data into three groups: normal (n = 15), impaired relaxation (n = 15), and pseudonormal (n = 30). One-way ANOVA or Kruskal-Wallis one-way ANOVA on ranks, where appropriate (based on whether normal distribution was present), were applied to test for statistical differences between the three groups. Paired comparisons were performed using the Bonferroni *t* test. Linear regression analysis was used to examine the relation between the Doppler and hemodynamic variables. Statistical significance was defined with $p \leq 0.05$.

RESULTS

Canine experiments. Table 1 summarizes the hemodynamic and Doppler changes in these experiments. Left ventricular filling pressures and EDV significantly increased ($p < 0.05$) while LV relaxation and global systolic function became worse ($p < 0.05$) after constriction of the circumflex coronary artery. The early diastolic transmitral pressure gradient was significantly lower ($p < 0.05$) and LV minimal pressure was significantly higher after circumflex constriction. The Ea significantly decreased as LV relaxation slowed. Importantly, the time interval $T_{Ea\text{-}E}$ was prolonged

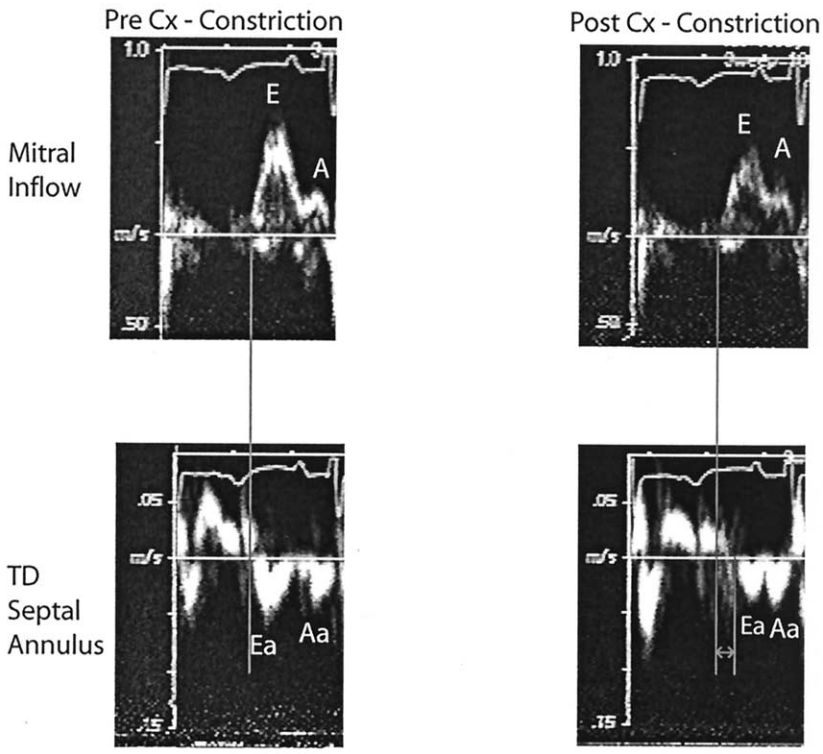

Figure 1. Mitral inflow and pulse wave tissue Doppler (TD) of the mitral annulus before and after constriction of the circumflex coronary artery (Cx). Notice the reduced velocity of Ea and its delayed onset with respect to onset of mitral E after the intervention. A = transmitral late diastolic velocity; E = transmitral early diastolic velocity.

(Fig. 1) under these settings. Inferior vena cava occlusion resulted in a significant decrease in Ea before, but not after, circumflex constriction, whereas its effect on the time interval was minimal under both circumstances. Significant correlations were observed between the time interval $T_{Ea\text{-}E}$ and each of tau (ranging from r = 0.78 at the septal side to r = 0.93 for the average duration) and LV minimal pressure (ranging from r = 0.75 at the septal side to r = 0.83 for the average duration) (Fig. 2). The relation between this time interval and each of tau and minimal pressure only in the stages with myocardial dysfunction was still significant (tau: r = 0.85, minimal pressure: r = 0.75, both $p < 0.05$).

Human studies. INITIAL POPULATION. In this population, there were 15 normal individuals as determined by their clinical status (no symptoms and no history of heart failure, hypertension, or coronary artery disease) and their echocardiographic and hemodynamic data (normal ventricular size, ejection fraction of 65%, lack of regional wall motion abnormalities, absence of valvular disease, and normal filling pressures and tau). These patients were in the intensive care

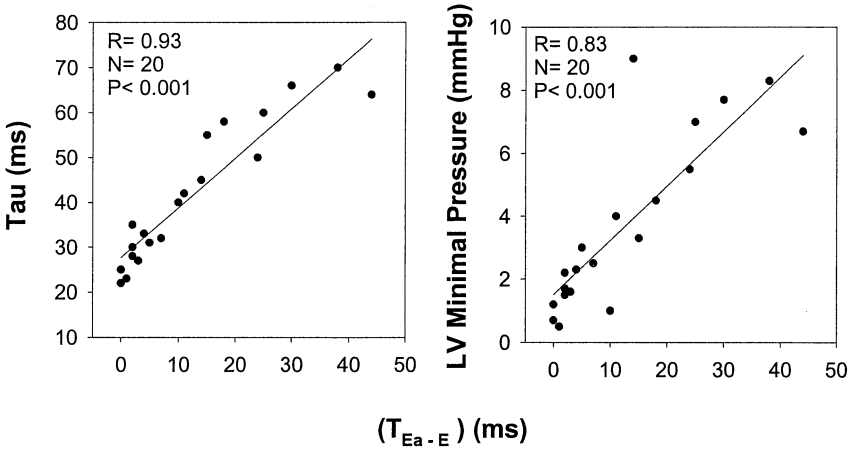

Figure 2. Regression plots between the average time interval between onset of Ea and onset of mitral inflow ($T_{Ea\text{-}E}$) and tau **(left)** and left ventricular (LV) minimal pressure **(right)**.

Table 2. Clinical and Hemodynamic Findings in the Initial Population

	Normal (n = 15)	IR (n = 15)	PN (n = 30)
Age (yrs)	63 ± 17	65 ± 15	62 ± 12
Heart rate (beats/min)	84 ± 15	82 ± 13	81 ± 13
Mean systemic arterial pressure (mm Hg)	87 ± 17	84 ± 19	84 ± 17
Mean pulmonary arterial pressure (mm Hg)	13 ± 3	20 ± 5	28 ± 6*
RAP (mm Hg)	5 ± 3	7 ± 4	14 ± 5.4*
Cardiac output (l/min)	5.5 ± 1.8	4.9 ± 1.5	4.6 ± 1.7
PCWP (mmHg)	12 ± 3	14 ± 5	21 ± 6*
Tau (ms)	34 ± 4.8	61 ± 10†	61 ± 11†
EDV (ml)	112 ± 27	126 ± 40	151 ± 45†
EF (%)	65 (58–70)‡	50 (35–66)	36.5 (27–45)
LA volume (ml)	35 ± 7	51 ± 13†	66 ± 27*

Data shown as mean ± SD or median (25th–75th percentile) where appropriate. *p < 0.05 vs. normal and impaired relaxation groups; †p < 0.05 vs. normal group; ‡p < 0.05 vs. impaired relaxation and pseudonormal groups.

EDV = end-diastolic volume; EF = ejection fraction; IR = impaired relaxation; LA = left atrium; PCWP = pulmonary capillary wedge pressure; PN = pseudonormal; RAP = mean right atrial pressure.

unit because of medical problems (pneumonia in six, sepsis in six, and bleeding in three). Based on the mitral inflow pattern, the other 45 patients were divided into two groups: impaired relaxation (ratio of transmitral early diastolic to late diastolic velocity [E/A ratio] <1; diagnosis: coronary artery disease in 10, idiopathic cardiomyopathy in five) and pseudonormal (E/A >1; diagnosis: coronary artery disease in 17, idiopathic cardiomyopathy in seven, and status post aortic valve replacement in six). There were no significant differences among the three patient groups regarding age or blood pressure. However, PCWP was significantly higher in patients with a pseudonormal pattern of mitral inflow. Mitral inflow, pulmonary venous flow parameters and TD

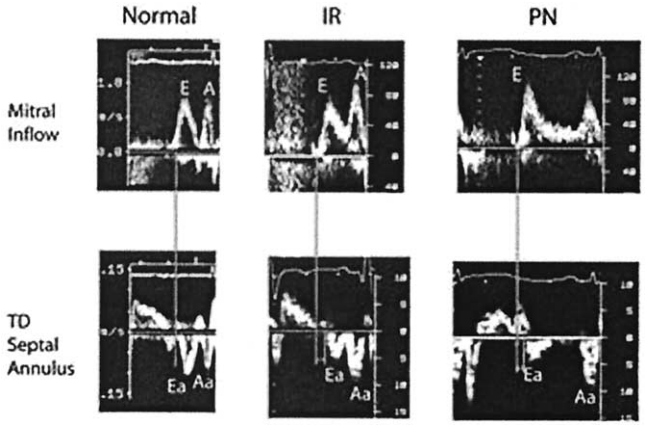

Figure 3. Mitral and tissue Doppler (TD) recordings of the mitral annulus from a normal, an impaired relaxation (IR), and pseudonormal (PN) patients. Notice the later onset of Ea with respect to onset of mitral E in the IR and PN patients.

velocities were also significantly different between the three groups. Tissue Doppler-derived time intervals readily differentiated patients with pseudonormal mitral inflow from normal subjects (Tables 2 and 3, Fig. 3). The $T_{Ea\text{-}E}$ was significantly related to tau ($r = 0.83$, $p < 0.001$, equation: $tau = 32 + 0.7\ T_{Ea\text{-}E}$) and the flow propagation velocity by color m-mode ($r = -0.6$, $p < 0.05$). Figure 4 shows the regression plot of PCWP by right heart catheterization versus PCWP by Doppler in all 60 patients (SEE = 2.8 mm Hg). In this group, the derivation of PCWP by Doppler was performed using $T_{Ea\text{-}E}$ in place of tau.

PROSPECTIVE POPULATION. Table 4 presents a summary of the clinical, hemodynamic, and Doppler data of this group. Two approaches were adopted to calculate mean PCWP in this group. In one approach, we directly substituted $T_{Ea\text{-}E}$

Table 3. Doppler Findings in the Initial Population

	Normal (n = 15)	IR (n = 15)	PN (n = 30)
E/A	1.1 (1–1.6)	0.7 (0.6–0.8)†	1.6 (1.2–2.2)*
DT (ms)	176 ± 54	223 ± 54‖	146 ± 38
SFF	0.47 ± 0.13	0.6 ± 0.1	0.45 ± 0.14‡
Ar-A (ms)	0 ± 20	7 ± 20	28 ± 10†
Lateral Ea (cm/s)	9 (8–10)§	6 (5–7.5)	5 (5–6.4)
Septal Ea (cm/s)	7 (6–8)§	6 (5–7.8)	5 (4–5.5)
Average Ea (cm/s)	8 (7.5–10)§	6 (5–7.65)	5 (4.5–6)
Average Aa (cm/s)	8.1 ± 3.4	8 ± 2.9	5.4 ± 2.2*
Lateral E/Ea	9.5 ± 1.5	9 ± 3	14 ± 5*
Septal E/Ea	10 (8.8–13)	10 (8.5–13)	18.2 (14–23)*
Average E/Ea	9.7 ± 2.7	10 ± 2.5	15.5 ± 4*
Lateral ($T_{Ea\text{-}E}$) (ms)	2 ± 4§	25 ± 7	30 ± 7
Septal ($T_{Ea\text{-}E}$) (ms)	3 (1–7)§	32 (22–54)	39 (15–59)
Anterior ($T_{Ea\text{-}E}$) (ms)	3.5 ± 8§	40 ± 11	37 ± 13
Inferior ($T_{Ea\text{-}E}$) (ms)	2.2 ± 8§	36 ± 10	38.6 ± 12
Average ($T_{Ea\text{-}E}$) (ms)	3.2 ± 5§	33 ± 8	37 ± 7.5

Data shown as mean ± SD or median (25th–75th percentile) where appropriate. *p < 0.05 vs. normal and impaired relaxation groups; †p < 0.05 vs. normal group; ‡p < 0.05 vs. impaired relaxation group; §p < 0.05 vs. impaired relaxation and pseudonormal groups; ‖p < 0.05 vs. normal and pseudonormal groups.

Aa = late diastolic velocity by tissue Doppler; Ar-A = difference between duration of Ar velocity in pulmonary venous flow and duration of transmitral A velocity; DT = deceleration time; E/A = ratio of transmitral early diastolic to late diastolic velocity; E/Ea = ratio of transmitral peak early diastolic velocity to mitral annulus peak Ea velocity by tissue Doppler; SFF = systolic filling fraction; $T_{Ea\text{-}E}$ = time interval between onset of Ea and onset of mitral inflow.

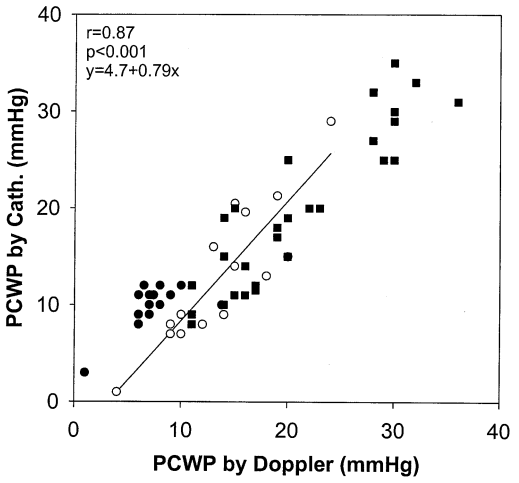

Figure 4. Regression plot of pulmonary capillary wedge pressure (PCWP) by right heart catheterization (Cath.) versus PCWP by Doppler in the initial group of 60 patients. Patients with normal relaxation are shown in **black circles**, those with impaired relaxation in **white circles**, and those with pseudonormal filling in **black squares**.

for tau in the analytic expression relating PCWP, IVRT, and left ventricular end-systolic pressure (LV_{es}). Figure 5 shows the correlation ($r = 0.84$, $p < 0.001$) between Doppler-derived PCWP and that obtained by right heart catheterization. The mean difference between Doppler and catheter PCWP was 1.3 ± 3.5 (range -5.5 to 5.4) mm Hg. In the second approach, we used the regression equation ($tau = 32 + 0.7\ T_{Ea\text{-}E}$) to derive tau from the Doppler time interval. Tau was then applied in the analytic expression along with IVRT and LV_{es} to predict PCWP ($r = 0.88$, $p < 0.001$, mean difference between Doppler and catheter PCWP $= 1 \pm 2.3$ mm Hg). Table 5 shows the results of the correlation between PCWP by catheterization and a number of Doppler parameters. Excluding normal patients ($n = 10$) resulted in an improvement in the relation between the E/Ea ratio and catheter PCWP (septal $r = 0.65$ to lateral $r = 0.76$; $p < 0.05$). However, excluding normal patients did not affect the correlation ($r = 0.79$) of PCWP derived noninvasively by Doppler ($PCWP_{Doppler}$) as predicted using $T_{Ea\text{-}E}$.

Table 4. Clinical, Hemodynamic, and Doppler Findings in the Prospective Population

Age (yrs)	61 ± 15
Heart rate (beats/min)	83 ± 12
Mean systemic arterial pressure (mm Hg)	85 ± 15
Mean pulmonary arterial pressure (mm Hg)	30 ± 10
Cardiac output (l/min)	5 ± 1.2
EF (%)	53 ± 17
EDV (ml)	133 ± 46
PCWP (mmHg)	19.5 ± 6.3
LA volume (ml)	70 ± 36
Mitral inflow: DT (ms)	194 ± 93
Mitral inflow: E/A	1.9 ± 1.4
Pulmonary venous: SFF	0.43 ± 0.14
Average Ea (cm/s)	7.4 ± 2.2
Average Aa (cm/s)	6.4 ± 2.9
Average E/Ea	14 ± 5.1
Average duration: ($T_{Ea\text{-}E}$) (ms)	35 ± 21

Data shown as mean ± SD.
EDV = end-diastolic volume; EF = ejection fraction; LA = left atrium; PCWP = pulmonary capillary wedge pressure. Other abbreviations as in Table 3.

Clinical application. In an attempt to simplify the method, we examined the relation of the ratio of IVRT/($T_{Ea\text{-}E}$) to PCWP. Catheter PCWP had a significant relation with the ratio ($r = -0.74$, $p < 0.01$, SEE = 4.4 mm Hg). In the initial group of 60 patients, a ratio of IVRT/($T_{Ea\text{-}E}$) <2 had a sensitivity of 80% and a specificity of 90% in identifying patients with PCWP >15 mm Hg. In the prospective group, a ratio <2 had a sensitivity of 91% and a specificity of 89% in detecting PCWP >15 mm Hg. Figure 6 shows the regression plot for the two populations combined. We also examined the clinical utility of the time interval measured at a single site of the mitral annulus. Similar sensitivity and specificity were noted using each individual site (sensitivity ranging from 70% to 76%, and specificity ranging from 71% to 78%) but with somewhat lower accuracy than the average value. The mean interobserver difference for Doppler-derived PCWP was 1.3 ± 0.5 mm Hg.

DISCUSSION

The canine experiments show the strong relation between the time interval $T_{Ea\text{-}E}$ and LV relaxation. The clinical study supports its use to identify patients with abnormal LV diastolic function irrespective of filling pressures. Furthermore, in conjunction with LV_{es} and IVRT, it can be used to predict PCWP. This was particularly useful in patients without cardiac disease where all other Doppler indexes were inaccurate.

Canine experiments. In the presence of normal myocardial function, myocardial expansion, annular recoil, and transmitral inflow occur in early diastole as the fast LV relaxation and diastolic suction lead to a rapidly declining LV pressure. With LV dysfunction, LV relaxation is slowed and delayed, and early diastolic suction is reduced (13). Accordingly, transmitral inflow becomes dependent on the increased left atrial pressure and transmitral pressure gradient (19). Under these situations, annular recoil in early diastole is delayed and follows the transmitral inflow. This may be related to the change in LV geometry and wall stress, whereby after myocardial dysfunction an increase in the ratio of end systolic meridional to circumferential wall stress occurs (20). The changes in wall stress may, in part, result in a reduced and delayed longitudinal fiber expansion. Importantly, the Doppler time interval changes were strongly related to the slowed LV relaxation, which is known to continue beyond the IVRT and into the later stages of LV filling in cardiac disease. Interestingly, in the presence of normal relaxation, preload reduction had no significant effect on the onset of Ea relative to onset of mitral E, unlike the peak Ea velocity, which showed a significant decrease.

Human studies. Impaired LV relaxation is frequently present in patients with a variety of cardiovascular disorders.

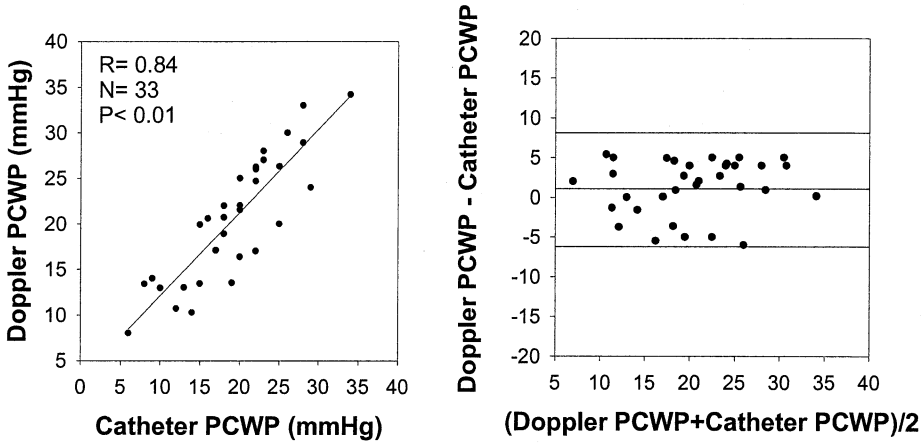

Figure 5. Regression plot between pulmonary capillary wedge pressure (PCWP) by catheter versus PCWP by Doppler **(left)** and the Bland Altman plot **(right)**. The **middle line** refers to the mean difference, and the **upper and lower lines** correspond to mean + 2 SD and mean − 2 SD, respectively.

Given its versatile and noninvasive nature, echocardiography is well-suited for the diagnosis of this abnormality. In this investigation, we show that the time interval $T_{Ea\text{-}E}$ can successfully detect patients with diastolic dysfunction irrespective of their LV filling pressures. This novel index is an important addition to the available two-dimensional (LV hypertrophy and LA volume) and Doppler parameters (difference between duration of Ar velocity in pulmonary venous flow and duration of transmitral A velocity [Ar-A], flow propagation velocity, and Ea) that can identify patients with a pseudonormal mitral inflow pattern. It also has several advantages including the very high feasibility of recording mitral inflow and annular velocities by TD (7) and the lack of effect of translation on its true value, unlike the situation with TD velocities. In addition, because ultrasound beam angulation decreases velocities but has no effect on the recording of onset of mitral E and Ea, this time interval can still be applied in patients where it is difficult to achieve proper alignment between the ultrasound beam and mitral flow or motion. Future studies are needed to examine the utility of this time interval in following the effect of medications and interventions on LV relaxation irrespective of their effect on filling pressures.

Table 5. Correlation Between Doppler Variables and Catheter PCWP in the Prospective Population

E/A	0.47*
DT	−0.4
IVRT	−0.57†
SFF	−0.58*
Ar-A	0.53*
Average Aa	−0.45*
Lateral E/Ea	0.66†
Septal E/Ea	0.45†
Average E/Ea	0.57†
IVRT/($T_{Ea\text{-}E}$)	−0.74*
$PCWP_{Doppler} = LV_{es} \times e^{-IVRT/(T_{Ea\text{-}E})}$	0.84†
$PCWP_{Doppler} = LV_{es} \times e^{-IVRT/tau}$	0.88†

*$p < 0.05$; †$p < 0.01$.
IVRT = isovolumetric relaxation time. Other abbreviations as in Tables 3 and 4.

Estimation of LV filling pressures. Left ventricular pressure at the time of mitral valve opening can be given by the equation (17,21): $PCWP = LV_{es} \times e^{-IVRT/tau}$, because pressure at mitral valve opening is very close to mean PCWP in the absence of mitral valve disease (a group of patients who were excluded from this study). We used a previously validated expression (18) to calculate LV_{es} along with IVRT as measured by Doppler and substituted tau with the time interval $T_{Ea\text{-}E}$. The use of $T_{Ea\text{-}E}$ was supported by the strong correlation observed with tau in the animal model and the initial population of 60 patients. In addition, one can actually derive tau from $T_{Ea\text{-}E}$ (see the preceding text) and then use the noninvasively derived tau for the Doppler prediction of PCWP; LV_{es} was entered in place of systolic blood pressure to avoid overestimation of

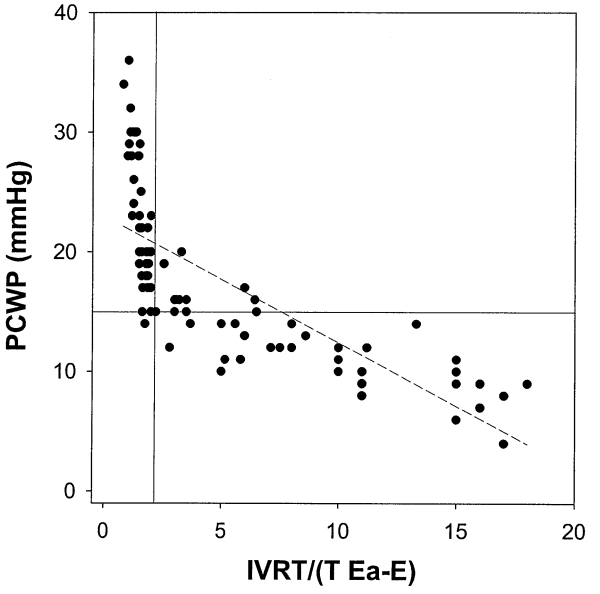

Figure 6. Regression plot between pulmonary capillary wedge pressure (PCWP) by catheter versus the dimensionless ratio of isovolumetric relaxation time (IVRT)/$T_{Ea\text{-}E}$ in all 93 patients. The **dashed line** is the regression plot line. The **vertical line** marks the IVRT/$T_{Ea\text{-}E}$ cutoff of 2, and the **horizontal line** marks the PCWP cutoff of 15.

PCWP when using the higher peak systolic pressure. The new method is particularly advantageous in normal subjects where the ratio of transmitral peak early diastolic velocity to mitral annulus peak Ea velocity by tissue Doppler (E/Ea ratio) can be inaccurate. In fact, the correlation of the E/Ea ratio with PCWP improved after the exclusion of patients without cardiovascular disease, whereas excluding these patients had no effect on the accuracy of the new approach. Furthermore, it is potentially more useful clinically in the group of patients with normal ejection fraction and diastolic dysfunction (not only those without cardiovascular disease) where the results of TD E/Ea are not as strong as in those with depressed ejection fraction. In fact, the current findings of E/Ea in patients with normal ejection fraction are similar to previous observations from our laboratory (6) and others (7) where a somewhat weaker relation between E/Ea and filling pressures (vs. stronger correlation in patients with reduced ejection fraction) is generally observed.

Study limitations. We excluded patients with mitral valve disease and those with prosthetic mitral valves. The utility of the new index remains to be examined in these patients. The clinical use of this time interval was not significantly improved by correcting for the heart rate (using the $\sqrt{}$R-R interval) given the relatively narrow range of heart rates of patients included in this study. However, patients with bradycardia, tachycardia, and atrial fibrillation were not included in this investigation, and the application of the time interval $T_{Ea\text{-}E}$ to them merits further studies. The $T_{Ea\text{-}E}$ may still be applicable in the presence of regular bradycardia or tachycardia and a single velocity pattern (mitral inflow and annulus velocities) because one is measuring the time to onset of E (and not to peak E) and to onset of Ea (and not to peak Ea). Measuring the interval from the R wave to peak E and to peak Ea could potentially lead to errors under these situations where a single waveform exists because the latter could be predominantly an A signal. The confidence intervals for the prediction of PCWP (around $\pm$7 mm Hg), which are similar to those obtained with other equations (5–7,13,16), should be considered when one is applying this approach. However, in equivocal studies where satisfactory pulmonary venous recording of Ar is not possible, and where Ea peak velocity is borderline, measuring this time interval could be helpful. While the equation used for calculating PCWP could be cumbersome for daily application, one can use the simple ratio of IVRT/($T_{Ea\text{-}E}$) to identify patients with PCWP >15 mm Hg.

Reprint requests and correspondence: Dr. Sherif F. Nagueh, 6550 Fannin Street, SM-1246, Houston, Texas 77030-2717. E-mail: sherifn@bcm.tmc.edu.

REFERENCES

1. Gorcsan J 3rd, Strum DP, Mandarino WA, Gulati VK, Pinsky MR. Quantitative assessment of alterations in regional left ventricular contractility with color-coded tissue Doppler echocardiography: comparison with sonomicrometry and pressure-volume relations. Circulation 1997;95:2423–33.
2. Isaaz K, Munoz del Romeral L, Lee E, Schiller NB. Quantification of the motion of the cardiac base in normal subjects by Doppler echocardiography. J Am Soc Echocardiogr 1993;6:166–76.
3. Oki T, Tabata T, Yamada H, et al. Clinical application of pulsed Doppler tissue imaging for assessing abnormal left ventricular relaxation. Am J Cardiol 1997;79:921–8.
4. Sohn D-W, Chai I-H, Lee D-J, et al. Assessment of mitral annulus velocity by Doppler tissue imaging in the evaluation of left ventricular diastolic function. J Am Coll Cardiol 1997;30:474–80.
5. Nagueh SF, Middleton KJ, Kopelen HA, Zoghbi WA, Quinones MA. Doppler tissue imaging: a noninvasive technique for evaluation of left ventricular relaxation and estimation of filling pressures. J Am Coll Cardiol 1997;30:1527–33.
6. Nagueh SF, Mikati I, Kopelen HA, Middleton KJ, Quinones MA, Zoghbi WA. Doppler estimation of left ventricular filling pressure in sinus tachycardia. Circulation 1998;98:1644–50.
7. Ommen SR, Nishimura RA, Appleton CP, et al. Clinical utility of Doppler echocardiography and tissue Doppler imaging in the estimation of left ventricular filling pressures: a comparative simultaneous Doppler-catheterization study. Circulation 2000;102:1788–94.
8. Nagueh SF, Sun H, Kopelen HA, Middleton KJ, Khoury DS. Hemodynamic determinants of the mitral annulus diastolic velocities by tissue Doppler. J Am Coll Cardiol 2001;37:278–85.
9. Garcia MG, Rodriguez L, Ares M, Griffin BP, Thomas JD, Klein AL. Differentiation of constrictive pericarditis from restrictive cardiomyopathy: assessment of left ventricular diastolic velocities in longitudinal axis by Doppler tissue imaging. J Am Coll Cardiol 1996;27:108–14.
10. Hasegawa H, Little WC, Ohno M, et al. Diastolic mitral annular velocity during the development of heart failure. J Am Coll Cardiol 2003;41:1590–7.
11. Baan J, Jong TTA, Kerkhof PLM, et al. Continuous stroke volume and cardiac output from intra-ventricular dimensions obtained with impedance catheter. Cardiovasc Res 1981;15:328–34.
12. Weiss JL, Frederiksen JW, Weisfeldt ML. Hemodynamic determinants of the time-course of fall in canine left ventricular pressure. J Clin Invest 1976;58:751–60.
13. Nishimura RA, Tajik AJ. Evaluation of diastolic filling of left ventricle in health and disease: Doppler echocardiography is the clinician's rosetta stone. J Am Coll Cardiol 1997;30:8–18.
14. Schiller NB, Shah PM, Crawford MH, et al. Recommendations for quantitation of the left ventricle by two-dimensional echocardiography: American Society of Echocardiography Committee on Standards, Subcommittee on Quantitation of Two-Dimensional Echocardiograms. J Am Soc Echocardiog 1989;2:358–67.
15. Kuecherer HF, Muhiudeen IA, Kusumoto FM, et al. Estimation of mean left atrial pressure from transesophageal pulsed Doppler echocardiography of pulmonary venous flow. Circulation 1990;82:1127–39.
16. Rossvoll O, Hatle LK. Pulmonary venous flow velocities recorded by transthoracic Doppler ultrasound: relation to left ventricular diastolic pressures. J Am Coll Cardiol 1993;21:1687–96.
17. Thomas JD, Flachskampf FA, Chen C, et al. Isovolumic relaxation time varies predictably with its time constant and aortic and left atrial pressure: implications for the noninvasive evaluation of ventricular relaxation. Am Heart J 1992;124:1305–13.
18. Kelly RP, Ting CT, Yang TM, et al. Effective arterial elastance as index of arterial vascular load in humans. Circulation 1992;86:513–21.
19. Ishida Y, Meisner JS, Tsujioka K, et al. Left ventricular filling dynamics: influence of left ventricular relaxation and left atrial pressure. Circulation 1986;74:187–96.
20. Douglas PS, Morrow R, Ioli A, Reichek N. Left ventricular shape, afterload and survival in idiopathic dilated cardiomyopathy. J Am Coll Cardiol 1989;13:311–5.
21. Gonzalez-Vilchez F, Ares M, Ayuela J, Alonso L. Combined use of pulsed and color M-mode Doppler echocardiography for the estimation of pulmonary capillary wedge pressure: an empirical approach based on an analytical relation. J Am Coll Cardiol 1999;34:515–23.